IJAREEIE

e-ISSN: 2278-8875
p-ISSN: 2320-3765

International Journal of Advanced Research in Electrical, Electronics and Instrumentation Engineering

Volume 13, Issue 5, May 2024

INTERNATIONAL STANDARD SERIAL NUMBER INDIA

Impact Factor: 8.317

| e-ISSN: 2278 – 8875, p-ISSN: 2320 – 3765| www.ijareeie.com | Impact Factor: 8.317|| A Monthly Peer Reviewed & Referred Journal |

||Volume 13, Issue 5, May 2024||

|DOI:10.15662/IJAREEIE.2024.1305001|

Fixed, Single, and Dual Axis Solar PV System Comparison with Dust Effect

Aouda Arfoa

Department of Electrical Power Engineering and Mechatronics, Tafila Technical University, Jordan

ABSTRACT: In this paper the performance and efficiency assessment of fixed, single-axis, and dual-axis solar photovoltaic power systems were studied. All three systems were installed in grid-connected configurations with identical power ratings of 6.0 kW and the same modules and inverters. All three systems were also physically implemented, and results were recorded for a complete one-year operation with two cases in one year with weekly cleaning and one year without cleaning. This paper will consider the comparison of the system with Dust. PVsyst Solar Simulator and MATLAB have been used to model and simulate the given system of the plant to check the accuracy level of recorded data from physical implementation, the effect of dust, and the cost have been calculated and evaluated. The energy produced, the energy lost, and the energy cost due to dust have been illustrated in graphical form. The PV system was studied by both simulation and actual physical installation.

KEYWORDS: PV System; Dual axis; Dust effect; PVsyst.

I. INTRODUCTION

For the last few years, research in photovoltaic-based energy generation specifically regarding solar tracking systems has become a hot topic. Moreover, studies are notable in both Asian countries and the United States [1, 2]. Since solar radiation data is usually presented as global radiation on a horizontal surface when the PV panels are positioned at an angle to the horizontal plane, the energy input to the PV system must be computed accordingly. The calculation is done in three phases, as mentioned in [3]. The first step uses data from the location to determine the diffuse and beam components of the global irradiation on the horizontal plane.

This is carried out by using(B0); the extraterrestrial daily irradiation of the sun, as a reference to calculating the ratio KT = G/B0; which is known as the clearness index, where B is the daily beam irradiation on the horizontal plane (W/m^2), B0is the he extraterrestrial daily irradiation (W/m^2), G represents the daily global irradiation on a horizontal plane, typically denoting the monthly average. Meanwhile, KT refers to the average attenuation of solar radiation by the atmosphere at a specific location during a particular month. In a subsequent step, the author cited in reference [3] employed an empirical approach to compute the diffuse irradiation. This approach states that the ratio of diffuse fraction (D) to global radiation (G) is a function of the clearness index KT. Here, D signifies the monthly average daily diffuse irradiation on a horizontal plane measured in watts per square meter. The described approach yields the beam irradiation on the horizontal plane as well as the diffuse irradiation; B represents the daily beam irradiation on a horizontal plane. In the third stage, the diffuse and beam irradiation on the sloped surface are calculated by considering the angular dependence of each component. The reflection of the surrounding area is also considered while evaluating the albedo. The percentage of radiation that reaches the ground and is reflected into the atmosphere is known as the albedo. As mentioned in reference [3], the receiver absorbs some of this reflected energy. As noted in reference [4], the three aforementioned components are combined to obtain the total daily irradiation on the sloped surface.

II. TRACKING SYSTEM

The main difference between an ideal PV cell and a practical PV device is the presence of resistances. A simple equivalent circuit model for a photovoltaic cell consists of a real diode in parallel with an ideal current source, see Figure 1. The ideal current source delivers current in proportion to the solar flux to which it is exposed. Where I is the current through the circuit, V is the voltage in the circuit, RS is the series resistance in the PV circuit, R_P is the parallel resistance in the PV circuit, I_{ph} is the reverse saturation current of the diode.

| e-ISSN: 2278 – 8875, p-ISSN: 2320 – 3765| www.ijareeie.com | Impact Factor: 8.317|| A Monthly Peer Reviewed & Referred Journal |

||Volume 13, Issue 5, May 2024||

|DOI:10.15662/IJAREEIE.2024.1305001|

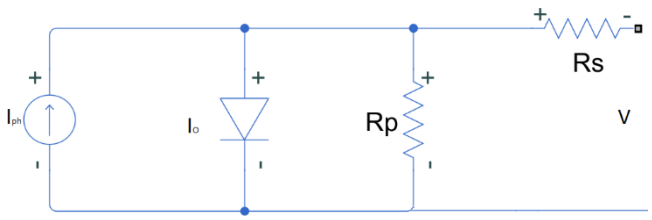

Figure 1. Equivalent circuit for PV cell.

Solar tracking can be implemented through the utilization of one-axis systems, and for enhanced precision, two-axis sun-tracking systems are employed. In the case of a two-axis tracking system, there exist two distinct types: azimuth/elevation (altitude-azimuth) tracking and polar (equatorial) tracking.

The tracker, an apparatus designed to maintain PV or photo-thermal panels in an ideal position perpendicular to the solar radiation throughout daylight hours, effectively amplifies the energy captured. Initially pioneered by Fibster in 1962, the first introduced tracker was entirely mechanical. A year later, Saavedra introduced a mechanism incorporating an automated electronic control, which was utilized for the orientation of an Apple pyrheliometer [5].

The presence of a solar tracker is not imperative for the functioning of a solar panel; however, its absence does result in a decline in performance. Even though solar trackers can amplify the energy acquisition of PV arrays, their installation entails certain considerations, including cost, dependability, energy consumption, upkeep, and performance.

All tracking systems possess some or all of the following characteristics:

- A singular column structure or one of the parallel console types.
- One or two motors that facilitate movement.
- A device that senses light.
- An energy supply that is either autonomous or auxiliary.
- Movement that corresponds to the path of light or follows a calendar.
- Movement that can be continuous or step-wise.
- Tracking that occurs throughout the year or excluding the winter season.
- The ability to adjust orientation with or without altering the tilt angle.

Passive tracking systems gracefully embrace the captivating principle of thermal expansion of matter, allowing them to elegantly pursue the sun without relying on the assistance of electronic control and motors. On the other hand, active solar trackers manifest as exquisite precision orientation systems that both enchant and astound, as they are rooted in the realms of either intricate mathematical calculations or the enchanting world of electro-optical sensors to find the exact position of the sun in the sky. After that, a controller turns on one or more actuators to move the panel into the ideal position. When using a single-axis tracker, all that needs to be changed to follow the sun's path from east to west is the azimuth angle. To achieve more accurate tracking, the system often compensates for variations in the sun's azimuth and height during the day. To enable the PV panel with two axes of rotation, each angle is adjusted with a single actuator. According to a number of comparative studies on the effectiveness of PV systems carried out in different geographic areas, the dual-axis solar tracker's yearly energy output is 5–10% and even up to 50% more than that of the single-axis and the fixed PV systems respectively [5–7].

The magnificent system of the tracker is constructed with a fundamental foundation, a remarkable set of sensors for the motion in the north and south direction, an extraordinary set of sensors for the motion in the east and west direction, and a mesmerizing photovoltaic panel.

Single-axis trackers, which are devices that rotate on one axis, move in a single direction either forward or backward. The axis of rotation for these trackers is typically aligned along a true north meridian. Various types of single-axis trackers exist, such as horizontal, vertical, tilted, and polar-aligned trackers, which rotate by their respective names [8].

The current structure is capable of identifying the existence of the sun and aligning the solar panel in the direction of the sun. The system automatically rotates the panel based on the position of the sun, maximizing the utilization of solar power. The single-axis module is composed of many components, including the motor driver, stepper motor, battery, logic circuit, charging circuit, control circuit, and solar panel. The dual-axis module rotates an extra axis to track the position of the sun by using an additional stepper motor and additional LDR sensors to detect light intensity. To track the movement of the sun from east to west, one DC motor is utilized, while another DC motor rotates the panel 300

| e-ISSN: 2278 – 8875, p-ISSN: 2320 – 3765| www.ijareeie.com | Impact Factor: 8.317|| A Monthly Peer Reviewed & Referred Journal |

||Volume 13, Issue 5, May 2024||

|DOI:10.15662/IJAREEIE.2024.1305001|

degrees to align it with the sun's direction. To distinguish between day and night, one LDR is used, and the other is used to determine the maximum light intensity. The subject controller receives the digital information from the two LDRs' output and uses it to operate the DC motors that adjust the panel. The microprocessor automatically de-energizes the motors when the panel is facing the sun. When a solar panel is put in an open area and exposed to sunlight, this model's implementation allows the panel's orientation to be automatically modified dependent on the position of the sun, which increases the panel's efficiency. A solar panel, regulator circuit, logic circuit, charging circuit, motor driver circuit, and control circuit make up the single-axis solar tracker module. The delay period given in the 8051 program is used by the microcontroller in the single-axis solar tracker module to rotate the panel. Maximal power production can be obtained by setting a suitable delay and syncing it with the position of the sun. The solar panel is moved for demonstration purposes by a DC motor that has an integrated reduction gear system, which follows the path of the sun from east to west. A small solar panel is connected to the motor shaft using the appropriate mechanism. The entire system, including the DC motor that powers the 3-watt solar panel, operates at 12V DC. This voltage is obtained from a 12V and 1.2Ah rated battery, which is charged by the solar panel itself [8]. The research examines a single-axis solar tracking system that revolves a photovoltaic panel around a slanted shaft. The motor is bidirectional and controlled by the true sun position, which is determined by two light-intensity sensors [9]. The two LDRs that make up the light sensors are positioned on opposite sides of the panel and are divided by an opaque plate. One of the two LDRs will be shadowed and the other will be lighted by the sun's rays, depending on their strength. A stronger signal will be produced by the LDR located on the side with higher sun ray intensity, while a lesser signal will be produced by the other. The PV panel will move in the direction of the highest solar radiation intensity thanks to the difference in output voltage between the two LDRs. The DC motor is controlled by a pulse signal sent to it by the PIC18F877A microprocessor. The motor may rotate in either a clockwise or counterclockwise direction thanks to a relay [10]. Dual-axis trackers are capable of moving in two different directions, allowing them to continuously face the sun. These trackers are designed to follow the sun both vertically and horizontally, thereby maximizing the generation of solar energy. Various implementations of dual-axis trackers exist, including tip-tilt and azimuth-altitude trackers [8].

In microprocessor and electro-optical sensor-based systems, the differential lighting of electro-optical sensors produces a differential control signal. The motor and apparatus are then oriented using this control signal, guaranteeing that the illumination of the sensors is uniform and balanced. Tilted plane mounting of the photodiodes can improve the photocurrent sensitivity. In concentrator PV applications, a collimating tube is often employed as a shading device to prevent the entry of diffuse irradiation, thereby enabling precise measurement of the sun's alignment position [11].

A sun-tracking system designed by Abdallah et al. relies on a mathematical definition of surface location that is based on the azimuth angle and the surface's slope. The slope is equal to the sun's zenith angle. Two tracking motors are used by the system; one rotates about the vertical axis and the other about the horizontal N-S axis. The daylight period is divided into 4- intervals, during which the solar and motor speeds are programmed into a PLC. Based on their predictions, the power consumed by the motors and control systems is expected to be less than 3% of the power saved by the tracking system. Two-axis tracking surfaces enhance daily collection by 41.34%, according to a study of the tracker's energy collection against a fixed surface inclined at 32.8 degrees [12, 13]. The author in [14] created a single-axis sun tracking system that increases a photo-voltaic module's daily output power using a programmable logic controller (PLC) unit. Two photo-resistive sensors are positioned apart, and one of them is shaded by a barrier. The sensor's resistance falls with increasing solar radiation intensity.

The PLC generates the appropriate output signal to activate an electromechanical sun-tracking device after comparing the output signals from the two sensors. The tracker scans in an east-west direction at an angle of around 120 degrees. A custom Visual Basic 5 software was created to monitor, control, and gather data from the PLC. The sun-tracker's performance was assessed and observed [14].

The microcontroller was designed, coded with an algorithm, and connected to an electrical board. They were able to achieve a maximum sensing resolution of around 68. They concluded that 99.98% of the maximum voltage is achieved if the PV module is positioned one degree from perpendicular. One can obtain 98.5% of the maximum value if it is 108° from the perpendicular [15]. To track the sun in azimuth and solar direction, Takeout designed and built a two-axis sun-tracking system using an 84-pin Xilinx XC95108 programmable logic device. DC motors are connected to a controller via an H-bridge construction. First, the angular steps and azimuth elevation ranges are calculated after the site has been chosen. There were twelve tilt steps in all. They also used code written in the Assembly or C++ languages to connect this tracking device to a PC for the purpose of monitoring the power generation. They came to the conclusion that the suggested solar tracker was adaptable and affordable [16, 17].

Hamilton developed and built a microcontroller-based sun-tracking device that tilted the array in two directions using two motors. The algorithm was created to read, amplify, and compare sensor inputs before digitally comparing the results to pinpoint the sun's precise location and turn on the unipolar stepper motors for positioning. The sensor was built like a four-sided pyramid, with solar cells affixed to each side. Programming for the microcontroller was done in C. A portable light source positioned at 16 points inside a spherical region was used to test the device in both the field

| e-ISSN: 2278 – 8875, p-ISSN: 2320 – 3765| www.ijareeie.com | Impact Factor: 8.317|| A Monthly Peer Reviewed & Referred Journal |

||Volume 13, Issue 5, May 2024||

|DOI:10.15662/IJAREEIE.2024.1305001|

and the lab. The outcomes demonstrated that throughout the day, the sun-tracking system collected the most energy, whereas the stationary system collected [19, 20].

III. METHODOLOGY

In order to learn more, a thorough energy and financial study of Fixed, Single, and Dual Axis Solar PV systems was carried out using both real-world installation and simulation.

3.1 PV system Specification and configuration

A 2kWp grid-connected photovoltaic system is selected in this paper, 6 modules, each 315Wp from JKM315P Poly-crystalline and inverter are used. All specifications of the PV module and inverter are shown in Table 1. A fixed, single, and dual-axis solar PV system with the specifications mentioned above is installed on the rooftop of Al Hussain Technical University as shown in Figure 2.

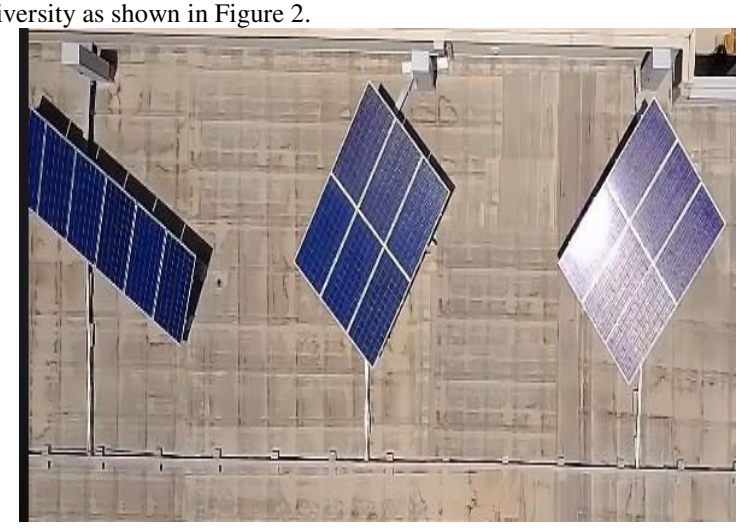

Figure 2 Installations of A Fixed, Single and Dual Axis Solar PV system.

Table 1. Specifications of PV Module and Inverter

Mechanical Characteristics					
Cell type	Poly-crystalline 156x156 mm (6 inch)				
No. of cells	72 (6X12)				
Dimensions	1956x992x40mm (77.01×39.05×1.57inch)				
Weights	26.5kg (58.4 lbs.)				
Specifications					
Module Type	JKM315P				
	STC		NOCT		
Maximum Power(Pmax)	315Wp		233Wp		
Maximum Power Voltage(Vmp)	37.2v		34.7v		
Maximum Power Current (Imp)	8.48A		6.71A		
Open-circuit Voltage(Vo.c)	46.2v		42.8v		
Short Circuit Current(Isc)	9.01A		7.28A		
Inverter Model	**1KVA**	**2KVA**	**3KVA**	**3KVA plus**	**5KVA**
Rated output power	1KVA/800w	2KVA/1.6KW	3KVA/2.4KW		5KVA/4KW
Output voltage wave form	Pure sine wave				
Output voltage regulation	230Vac±5%				
Output frequency	50Hz				
Peak efficiency	93%				
Overload protection	5s@≥150%;10s@110%~150%load				
Surge Capacity	2*rated power for 5 second				
Nominal DC input voltage	12Vdc	24Vdc	24Vdc		48Vdc
Cold start voltage	11.5Vdc	23.0Vdc	23.0Vdc		46.0Vdc
High DC recovery voltage	15Vdc	30Vdc	32Vdc		62Vdc
High Dc-cut off Voltage	16Vdc	31Vdc	33Vdc		63Vdc
No load power Consumption	<25w				<55w

| e-ISSN: 2278 – 8875, p-ISSN: 2320 – 3765| www.ijareeie.com | Impact Factor: 8.317|| A Monthly Peer Reviewed & Referred Journal |

||Volume 13, Issue 5, May 2024||

|DOI:10.15662/IJAREEIE.2024.1305001|

3.2 Geographical and Meteorological Data

To get accurate data regarding geographical and irradiance data we installed a meteorological station on the same place as the PV solar system. The irradiation and temperature of the selected site is shown in Figure 3.

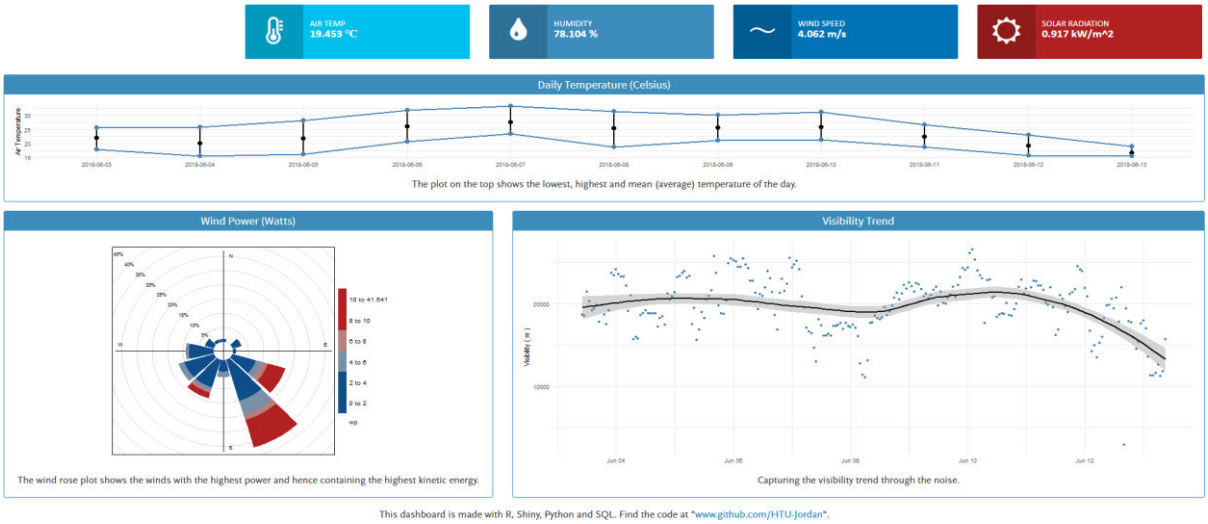

Figure 3 Geographical and Irradiance Data.

IV. ANALYSIS AND SIMULATION USING PVSYST AND MATLAB

Both PVsyst and Matlab facilitate the implementation of power system networks under various operating conditions and accurately simulate the obtained results as if they were derived from real-life applications. This not only saves significant time and money but also enhances safety. The objective of this study is to obtain precise measurements from all systems for comparison with simulation outcomes. To mitigate power losses in the system, tracking systems were incorporated into the power system design in PVsyst.

Furthermore, single tracking and dual tracking were added to the system. The design of the tracking system was acquired by tracking solar radiation and reducing the shaded area. Simulation results of all three systems are summarized in Table 2 which shows the results of the generated energy values of the system (6KW) for each part by using fixed tilt, single, and dual. Table 3 illustrates the disparity in shading factor between the actual system and the simulated system produced by PVsyst. After the desired parameters were inserted in Excel's schematic, the simulation was found to be working correctly as shown in Figure 4.

Table 2 Energy expected to be produced by HTU PV system plant.

Months	Fixed Tilt kWh	Single Axis kWh	Dual Axis kWh
January	673.2	720.6	967.5
February	752.1	778.2	907.5
March	876.9	878.7	1008.9
April	819.3	835.2	1065.3
May	826.8	889.5	1101.9
June	803.1	893.4	1068.6
July	738	807.9	907.5
August	801	834.3	992.4
September	859.5	860.1	1090.8
October	752.1	761.1	990.9
November	688.2	728.7	975
December	661.5	699.9	961.2
Year	9282	9735	12036

| e-ISSN: 2278 – 8875, p-ISSN: 2320 – 3765| www.ijareeie.com | Impact Factor: 8.317|| A Monthly Peer Reviewed & Referred Journal |

||Volume 13, Issue 5, May 2024||

|DOI:10.15662/IJAREEIE.2024.1305001|

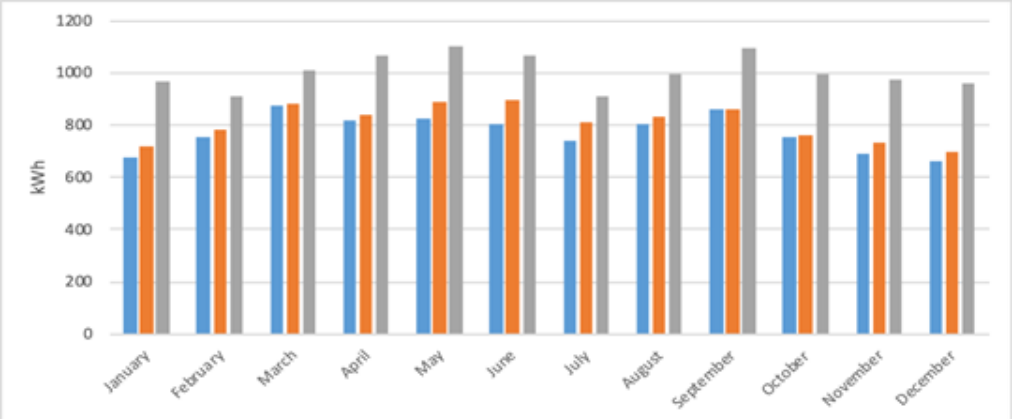

Figure 4 Simulation Results of Fixed Tilt, Single Axis and Dual Axis using PVsys.

Table 3 Shading Factor for Fixed Tilt, Single Axis and Dual Axis.

Azimuth/Height	90°	80°	70°	60°	50°	40°	30°	20°	10°	2°
–180°	0	0.012	0.064	0.124	0.196	0.294	0.444	0.277	0	0
–160°	0	0.08	0.05	0.058	0.117	0.132	0.127	0.044	0.042	0.043
–140°	0	0	0.03	0.052	0.063	0.08	0.124	0.111	0.059	0.025
–120°	0	0	0.007	0.019	0.029	0.086	0.197	0.335	0.329	0.237
–100°	0	0	0	0	0.004	0.02	0.161	0.334	0.497	0.573
–80°	0	0	0	0	0.008	0.026	0.118	0.253	0.41	0.552
–60°	0	0.013	0.011	0.009	0.002	0.007	0.057	0.092	0.163	0.263
–40°	0.26	0.015	0.006	0.002	0	0	0.017	0.031	0.073	0.131
–20°	0	0	0	0	0	0	0.005	0.043	0.086	0.129
0	0	0	0	0	0	0	0	0.57	0.135	0.203
20°	0	0	0	0	0.002	0	0.005	0.043	0.089	0.129
40°	0.026	0.015	0.006	0.002	0.008	0.07	0.017	0.031	0.135	0.131
60°	0.016	0.013	0.011	0.009	0	0.026	0.057	0.092	0.089	0.026
80°	0	0	0	0	0.008	0	0.118	0.253	0.41	0.552
100°	0	0	0	0	0.004	0.02	0.161	0.334	0.497	0.057
120°	0	0	0.007	0.019	0.029	0.086	0.197	0.335	0.329	0.237
140°	0	0	0.03	0.052	0.063	0.08	0.124	0.111	0.059	0.025
180°	0	0.08	0.05	0.088	0.117	0.132	0.127	0.094	0.042	0.043
160°	0	0.012	0.064	0.124	0.196	0.294	0.444	0.277	0	0

Figures 5 and 6 depict a simplified schematic of the I-V curve system for a design system utilizing MATLAB I-V. The utilization of characteristic curves serves as a tool to ascertain and comprehend the fundamental parameters of a component or device. Furthermore, these curves can also be employed to mathematically model the behavior of said component or device within an electronic circuit. However, similar to most electronic devices, there exists an infinite number of I-V characteristic curves that represent the diverse inputs or parameters. Consequently, we have the capability to exhibit a collection or set of curves on a single graph in order to illustrate the various values.

| e-ISSN: 2278 – 8875, p-ISSN: 2320 – 3765| www.ijareeie.com | Impact Factor: 8.317|| A Monthly Peer Reviewed & Referred Journal |

||Volume 13, Issue 5, May 2024||

|DOI:10.15662/IJAREEIE.2024.1305001|

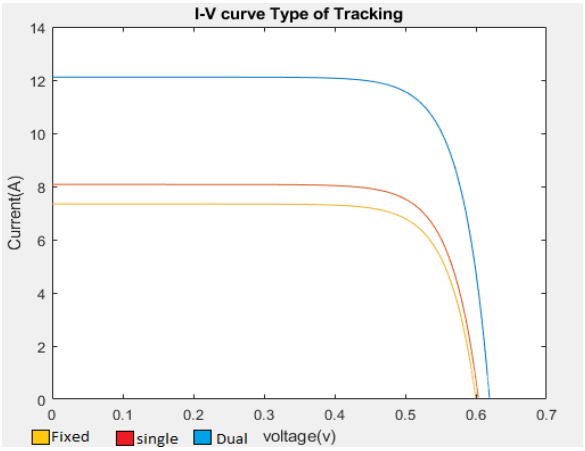

Figure 5. I-V characteristic of Fixed Tilt, Single and Dual.

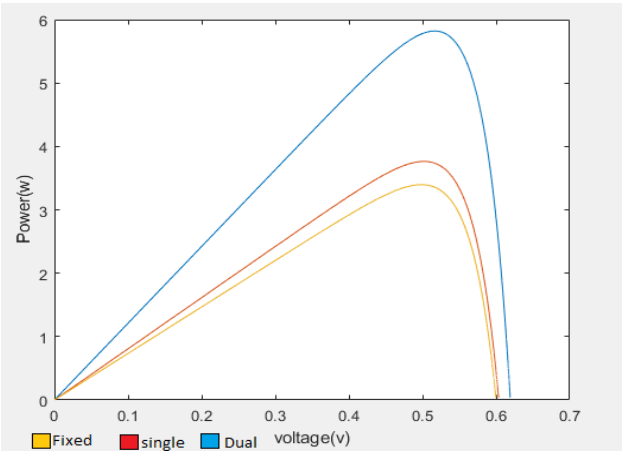

Figure 6. The power curve of Fixed Tilt, Single and Dual.

In this paper fixed, single, and dual-axis solar tracker systems were simulated, and energy generation of a full year was calculated for the three physical systems. The results measured by the physical installation of three systems are presented in Table 4.

Table 4 Real-time energy result with a cleaned system for Fixed Tilt, Single and Dual.

Months	**Fixed Tilt** (kWh)	**Single Axis** (kWh)	**Dual Axis** (kWh)
January	685.86	755.88	924
February	778.08	809.61	866.7
March	830.04	869.07	963.6
April	759.96	799.2	1017.3
May	767.85	861.75	1052.4
June	746.79	837.72	1020.6
July	676.59	761.67	866.7
August	743.97	777.6	947.7
September	770.61	809.85	1041.6
October	725.88	770.76	946.2
November	652.41	697.2	931.2
December	614.4	660.9	918
Year	8752.44	9411.21	11496

These data are based on cleaning panels. We carried out weekly cleanings. The difference in data between the simulation and real installation for fixed tilt is 5.3%,3.2% for the single axis, and 5.5 for the dual axis. To consider the dust effect for all systems, the data were collected from the physical installation for a full year without cleaning any of the panels. The total result is shown in Table 5. As shown in Figure 7, the total energy lost in the fixed system was found to be 376.8 kWh, for a year which costs around $63. For the single axis, the total energy lost was 320.2 kWh, for a year that costs around $54. For the dual axis, the total energy lost was 233.77kWh, for a year that costs around $39, see Figure 8. Table 5, Table 6, and Table 7 show the cost of the energy lost by the effect of dust on each solar panel system. We note that the different costs of energy lost between the fixed-axis system and dual-axis system will cover the cost of the tracking system mechanism.

| e-ISSN: 2278 – 8875, p-ISSN: 2320 – 3765| www.ijareeie.com | Impact Factor: 8.317|| A Monthly Peer Reviewed & Referred Journal |

||Volume 13, Issue 5, May 2024||

|DOI:10.15662/IJAREEIE.2024.1305001|

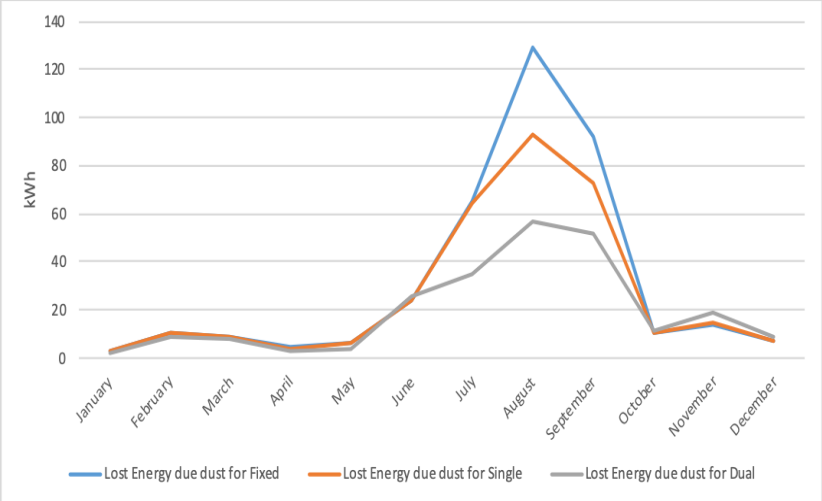

Figure 7. Lost Energy due dust effect.

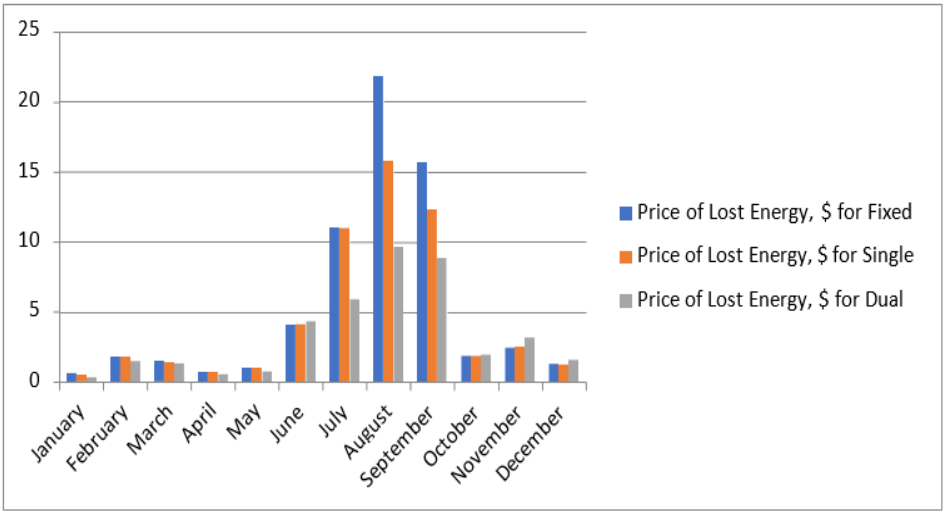

Figure 8. Cost of the Lost Energy by the Effect of Dust

Table 5 Real-time energy result without cleaned system for Fixed Tilt, Single and Dual.

Months	Fixed Tilt with dust (kWh)	Single Axis with dust (kWh)	Dual Axis with dust (kWh)
January	682.4307	752.85648	922.152
February	767.18688	799.08507	858.033
March	820.90956	860.3793	955.8912
April	755.40024	795.204	1014.2481
May	761.7072	855.71775	1048.1904
June	722.89272	813.42612	995.085
July	611.63736	696.92805	832.032
August	615.26319	684.288	890.838

| e-ISSN: 2278 – 8875, p-ISSN: 2320 – 3765| www.ijareeie.com | Impact Factor: 8.317|| A Monthly Peer Reviewed & Referred Journal |

||Volume 13, Issue 5, May 2024||

|DOI:10.15662/IJAREEIE.2024.1305001|

September	678.1368	736.9635	989.52
October	714.9918	759.96936	934.8456
November	638.05698	682.5588	912.576
December	607.0272	653.6301	908.82
Year	8375.64063	9091.00653	11262.2313

Table 6 Lost Energy due dust effect.

Months	Lost Energy due to dust for Fixed (kWh)	Lost Energy due to dust for Single (kWh)	Lost Energy due to dust for Dual (kWh)
January	3.429	3.023	1.848
February	10.89312	10.52493	8.667
March	9.130	8.690	7.7088
April	4.559	3.996	3.0519
May	6.142	6.032	4.2096
June	23.89728	24.29388	25.515
July	64.95264	64.74195	34.668
August	128.70681	93.31	56.862
September	92.47	72.88	52.08
October	10.88	10.79064	11.354
November	14.35302	14.64	18.624
December	7.372	7.269	9.18
Year	376.79937	320.20347	233.76

Table 7 Cost of The Lost Energy by The Effect of Dust.

Months	Price of Lost Energy, JOD for Fixed **($)**	Price of Lost Energy, JOD for Single **($)**	Price of Lost Energy, JOD for Dual **($)**
January	0.581237	0.5124	0.3132
February	1.846292	1.7838	1.4689
March	1.547532	1.473	1.3065
April	0.772841	0.6772	0.5172
May	1.041153	1.0224	0.7134
June	4.050386	4.1176	4.3245
July	11.00892	10.973	5.8759
August	21.81471	15.815	9.6376
September	15.67342	12.353	8.8271
October	1.845458	1.8289	1.9244
November	2.432715	2.4815	3.1566
December	1.249627	1.2321	1.5559
Year	63.8643	54.271	39.621

|e-ISSN: 2319-8753, p-ISSN: 2347-6710| www.ijirset.com | Impact Factor: 8.423| A Monthly Peer Reviewed & Refereed Journal |

|| Volume 13, Issue 5, May 2024 ||

| DOI:10.15680/IJIRSET.2024.1305001 |

V. CONCLUSION

In this paper 6kWp fixed, single, and dual-axis solar collection systems are compared with and without the Dust Effect. Using this comparison, the effect of dust and financial losses were calculated and assessed. The total of the lost energy from cleaned and uncleaned fixed systems is expected to be 376.79 kWh a year. That equals around $63. The total of the lost energy from the cleaned and uncleaned single tracking system is expected to be 320.2 kWh a year which costs around $54. The total of the lost energy from cleaned and uncleaned dual tracking systems is expected to be 233.7 kWh a year which costs around $39. We note the difference in cost of lost energy between fixed and dual systems will cover the cost of the tracking system mechanism, It is recommended to use a tracking system instead of a fixed one to decrease the dust effect, the tracking system will help to reduce the dust effect by around 50%.

REFERENCES

[1] Qais H. Alsafasfeh, Omar A. Saraereh, Imran Khan and Sunghwan Kim", Solar Power System Power flow analysis, Sustainability, 11(6), 1744, 2019.
[2] A Eial Awwad, On the perspectives of SiC MOSFETs in high-frequency and high-power isolated DC/DC converters, Universitätsverlag der TU Berlin, 2018
[3] Nadeem Asgher, Tariq Iqbal, Design and Simulation of a Floating Solar Photovoltaic System for an Offshore Aquaculture Site in Canada, JJEE Vol. 9, No. 4, 2023, pp. 466-480.
[4] Markvart T. Solar electricity, 2nd ed., New York: John Wiley and Sons Inc.;1996.
[5] Roth P, Georgiev A, Boudinov H.," Cheap two-axis sun following device", Energy Conversion and Management, 46:1179–92, 2005.
[6] Kvasznicza Z, Elmer G.," Optimizing solar tracking systems for solar cells" ,4th Serbian–Hungarian joint symposium on intelligent systems; 2006.
[7] Poulek V, Libra M. New bifacial solar trackers and tracking concentrators; 2007. http://www. solar- trackers.com.
[8] Online Resource: Types of Solar Trackers, http://Greenworldinvestor.com.
[9] Elmehdi Nasri, Tarik Jarou, Jawad Abdouni, Younes El Koudia, Enhancing Energy Reliability and Balance with Fuzzy Logic Controlled Microgrid System, JJEE Vol. 9, No. 4, 2023, pp. 591-606
[10] A Eial Awwad, Dynamic performance enhancement of a direct-driven PMSG-based wind turbine using a 12-sectors DTC, World Electric Vehicle Journal 13 (7), 123, 2022.
[11] Heredia I.L., Moreno J.M., Magalhaes P.H., Cervantes R., Que´me´ re´ G., Laurent O.. "Inspira's CPV sun tracking (concentrator photovoltaics)" Springer; p. 221–51, 2007.
[12] Abdallah S, Nijmeh S.," Two axes sun tracking system with PLC control", Energy Conversion and Management,45:1931–9, 2004.
[13] Kidist Berhane Zergaw, Milkias Berhanu Tuka, Analysis of Voltage Dip Impact on Doubly Fed Induction Generator under Dynamic Conditions, JJEE Vol. 9, No. 3, 2023, pp. 338-356.
[14] Al-Mohamad A.," Efficiency improvements of photo-voltaic panels using a sun trackingsystem", Applied Energy; 79:345–54,2004
[15] Peterson T, Rice J,Valane J. Solar tracker; 2005. http://ltc.cit.cornell.edu/courses/ee476/FinalProjects/s2005/tp62/website/solartracker
[16] Lakeou S, Ososanya E, Latigo BO, Mahmoud W, Karanga G, Oshumare W.," Design of a low-cost digital controller for a solar tracking photo-voltaic (PV) module and wind turbine combination system", 21st European PV solar energy conference; 2006.
[17] Lakeou S, Ososanya E, Latigo BO, Mahmoud W.,"Design of a low-cost solar tracking photo-voltaic (PV) module and wind turbine combination system", 21st European Photovoltaic Solar Energy Conference, 4–8 September, 2006, Dresden, Germany.
[18] Hamilton SJ. Sun-tracking solar cell array system. Bachelor of Engineering Thesis Division of Electrical Engineering. Department of Computer Science & Electrical Engineering, University of Queenzland; October 1999.
[19] Pouya Derakhshan Barjoei, Mehrdad Tavasoli-Kouhpaei, Optimal Design of Fuzzy Controller for Photovoltaic Maximum Power Tracking Using Particles Swarm Optimization Algorithm, JJEE Vol. 9, No. 3, 2023, pp. 439-449.
[20] M. Louy, Q. Tareq, S. Al-Jufout, Q. Alsafasfeh, and C. Wang, "Effect of dust on the 1-MW photovoltaic power plant at Tafila Technical University," IEEE International Renewable Energy Congress, pp. 1-4, 2017.

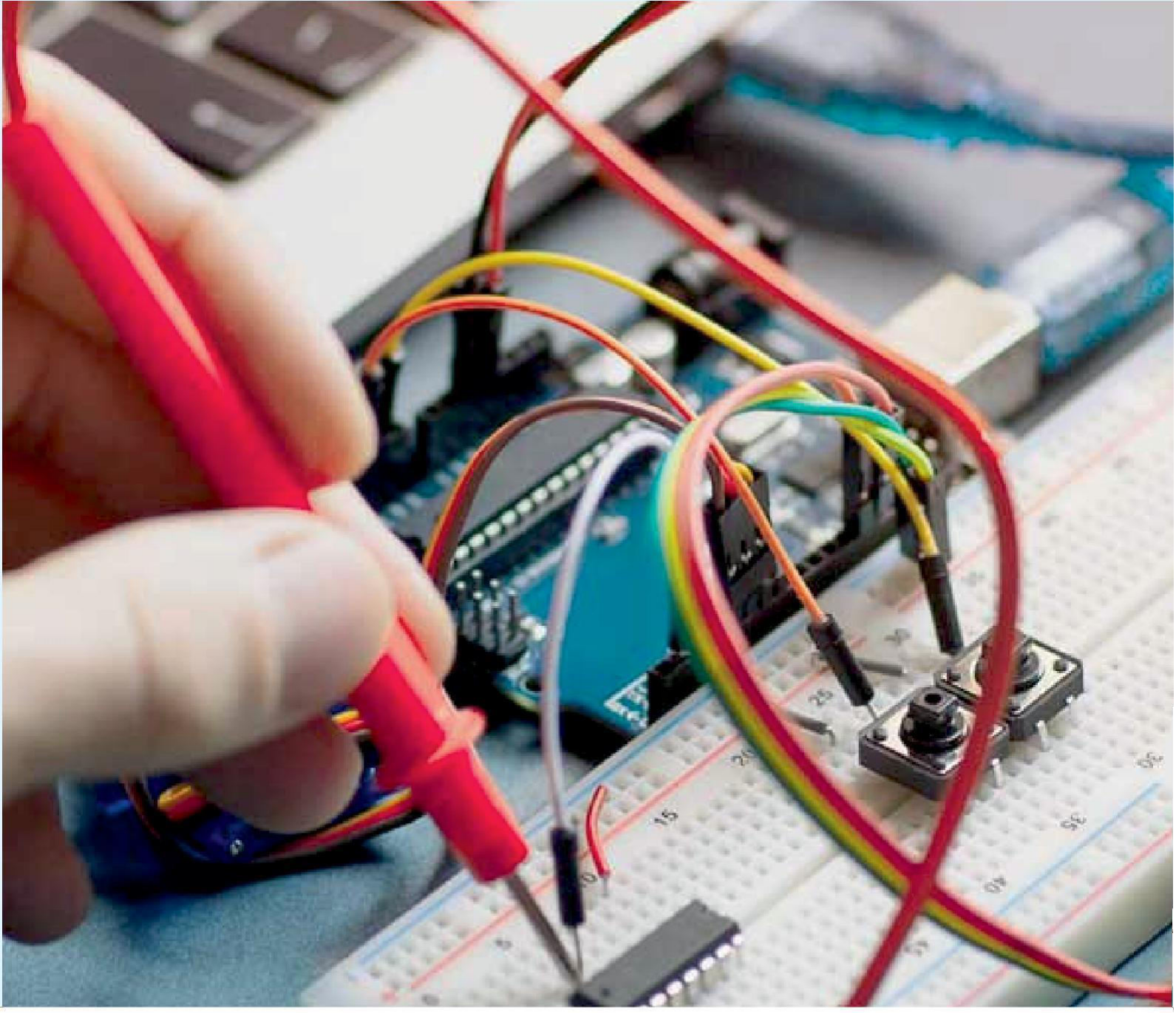

INNO SPACE
SJIF Scientific Journal Impact Factor

doi cross ref

ISSN INTERNATIONAL STANDARD SERIAL NUMBER INDIA

निस्केयर NISCAIR

International Journal of Advanced Research

in Electrical, Electronics and Instrumentation Engineering

9940 572 462 6381 907 438 ijareeie@gmail.com

Scan to save the contact details